

Partitioning of a Polymer Chain between Two Confining Cavities: The Roles of Excluded Volume and Finite Size Conduits

Stefan Tsonchev and Rob D. Coalson

Department of Chemistry

University of Pittsburgh

Pittsburgh, PA 15260

Abstract: Lattice-field calculations are performed on a Gaussian polymer chain confined to move within the region defined by two fused spheres. The results of the calculations are in accord with recent experimental measurements and computer simulations, and suggest that current theoretical understanding of polymer partitioning phenomena is not adequate when excluded volume interactions between the monomers are present. It is also shown that the notion of ground state dominance can fail even in the large monomer limit.

PACS numbers: 61.82.Pv, 83.70.Hq, 05.90.+m

A number of technologically important processes such as gel electrophoresis, size exclusion chromatography and membrane separation [1] depend on the partitioning of a polymer chain between two or more confining cavities connected by small conduits. The goal is to utilize the dependence of the partitioning on molecular properties such as polymer length or, in the case of polyelectrolytes, electrical charge and electrolyte composition, to selectively separate polymer chains, e.g. according to their molecular weight.

Current theoretical understanding of polymer partitioning via the principles of equilibrium statistical mechanics [2, 3] is based on the following notions. The Helmholtz free energy A of a polymer chain of length M is estimated as $\beta A \cong M(b/R)^{1/\nu}$, where $\beta^{-1} = kT$, b is the Kuhn length of the polymer, R is the characteristic linear dimension of the cavity, and $\nu = 1/2, 3/5$ for chains without and with excluded volume, respectively. The argument then goes that if two cavities with different sizes are connected by a narrow conduit (such that thermal equilibrium is established between them), the polymer chain will partition itself such that the ratio of the number of monomers in each cavity (designated 1 and 2) is:

$$K \equiv \frac{M_1}{M_2} = \exp[-\beta(A_1 - A_2)] \cong \exp\left[-(\text{const})M\left(\frac{1}{R_1^{1/\nu}} - \frac{1}{R_2^{1/\nu}}\right)\right], \quad (1)$$

where *const* is a constant of order unity. This leads immediately to the conclusion that the polymer prefers to occupy the larger cavity (say, cavity 1), and in particular that $\ln K$ grows linearly with the polymer chain length.

There are several approximations involved in arriving at Eq. (1). The estimation of $\beta A_{1,2}$ assumes that ground state dominance of the Green's function governing the distribution of monomers associated with the polymer [4] applies. Naively, this requires that the polymer chain in cavity 1,2 be sufficiently long that $\beta A_{1,2} \gg 1$ (but see below). Furthermore, incorporating the effects of excluded volume by modifying the exponent ν from the value of 1/2 (valid for a simple Gaussian chain [4]) to 3/5 requires the application of rough scaling arguments.

Eq. (1) seems intuitively reasonable when excluded volume effects are suppressed, because the polymer chain gains entropy when it passes from the smaller to the larger sphere. However, when excluded volume is included, intuition suggests that there will be a point beyond which putting more monomers in the larger sphere will cost, rather than lower, free energy, due to inter-monomer repulsion. Indeed, recent experimental partition coefficient measurements indicate the existence of such a saturation effect. In these experiments [5] a large (100 nm) spherical cavity was etched into a gel polymer network. Pockets in the gel network, typically 5–10 nm in linear dimension, play the role of the “small” cavity in the above arguments. $\ln K$ was indeed found to grow nearly linearly with M for small M , but a slower (sublinear) growth rate was observed as M was increased.

Recent Langevin dynamics simulations on a model of this gel/cavity system show similar effects [6]. The simulations also indicate a monotonic increase in $\ln K$ with M , followed by a turnover regime (as excluded volume effects become significant). At large M , $\ln K$ was found in the simulations to *decrease* with M . Clearly, intuition, experiments and simulations all suggest that Eq. (1) needs to be modified when excluded volume effects become significant.

In this letter we consider the equilibrium partitioning ratio of a Gaussian polymer chain in a container comprised of two spheres of different radii connected by a small aperture (cf. Fig. 1). When excluded volume effects are neglected, numerically exact calculations

of the monomer density in either sphere can be performed by solving an appropriate three-dimensional (3D) Schrödinger Equation. We have carried out such calculations using simple real-space lattice methodology. When excluded volume is included, a mean-field solution can be obtained by solving the same Schrödinger Equation with a modified effective potential that depends self-consistently on the monomer density. We have also carried out calculations of this type. These shed light on both the no-excluded volume limit and the effect of significant excluded volume. We also study the effect of aperture size on the results. The limit of an infinitesimal aperture, which allows thermal contact and material transfer without significantly altering the topologies of the two individual spheres, is conceptually important but not necessarily experimentally realistic. Finite size apertures are found to modify the behavior of the system significantly in some respects. For the case of a single polymer represented via the Gaussian Chain Model, the equilibrium properties are completely determined in the absence of intermonomer excluded volume interactions by the eigenfunctions and eigenvalues of the following 3D Schrödinger Equation [4]:

$$\left[-\frac{b^2}{6}\nabla^2 + V(\vec{r})/kT \right] \psi(\vec{r}) = E\psi(\vec{r}) . \quad (2)$$

Here $V(\vec{r})$ is an externally supplied potential energy function experienced by each monomer in the polymer. In the present case V is zero inside the container and infinite at the container walls. Thus, the effective quantum mechanical problem is that of a particle in the box indicated in Fig. 1. Determination of the eigenvalues/vectors for this problem must be done numerically. Although the system shown in Fig. 1 has cylindrical symmetry, we have chosen to develop a numerical method for solving the Schrödinger Equation which is valid for arbitrary 3D bound state problems. Specifically, we use a finite-difference position space representation, in which the wavefunction is described on a cubic real space lattice [7]. In this representation the potential energy matrix is diagonal (with diagonal value equal to the value of the potential at a given lattice point) and the kinetic energy entails off-diagonal coupling between nearest neighbors, as prescribed by simple symmetric finite-differencing of the Laplacian. Since the overall Hamiltonian matrix is sparse, low lying energy eigenfunctions and eigenvectors can be computed efficiently via a Lanczos algorithm [8].

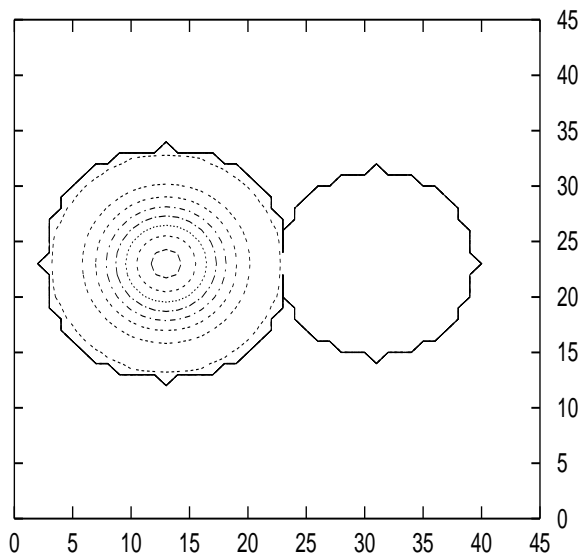


Figure 1: Slice through a plane containing the symmetry axis of two spheres with radii $R_1 = 1.0$ (left) and $R_2 = 0.8$ (right) connected by a narrow (“minimally-fused”) aperture. (Imperfections in the shape of the confining container are lattice artifacts.) Solid line shows outline of the confining system. Also shown, via dashed lines, is a contour plot of $\psi_0^2(\vec{r})$ in this plane for the case of $\lambda = 0.0$ (no excluded volume). Note that this function is completely confined to the large sphere.

Given the eigenvalues E_j and unit-normalized eigenfunctions ψ_j of the Schrödinger Equation (2), the monomer density can be synthesized as:

$$\rho(\vec{r}) = \frac{\sum_{j=0}^{\infty} \sum_{k=0}^{\infty} A_j A_k \psi_j(\vec{r}) \psi_k(\vec{r}) f(M; E_j, E_k)}{\sum_{j=0}^{\infty} A_j^2 e^{-ME_j}}, \quad (3)$$

where $A_j = \int d\vec{r} \psi_j(\vec{r})$, and

$$f = \begin{cases} \frac{e^{-ME_j} - e^{-ME_k}}{E_k - E_j} & ; \text{for } E_j \neq E_k \\ M e^{-ME_j} & ; \text{for } E_j = E_k \end{cases}. \quad (4)$$

The f factors suppress high-lying excited states (more quickly as M increases), so that the sums in Eq. (3) can be truncated at a finite value using the information obtained via diagonalization of a finite-dimensional Hamiltonian matrix associated with a particular lattice size.

Since the energy levels E_j are independent of M when the potential energy function $V(\vec{r})$ is externally prescribed, the condition $M(E_1 - E_0) \gg 1$ is guaranteed for long polymer chains. In this limit ground state dominance occurs, i.e., only the ground state of the Hamiltonian in Eq. (2) affects the thermodynamics of the system, and in particular $\rho(\vec{r}) \rightarrow M\psi_0^2(\vec{r})$.

Results of calculations for the parameters $R_1 = 1.0$, $R_2 = 0.8$ and $b = 0.2$ for a polymer confined to the volume of two spheres sharing one common point on the lattice are shown in Figs. 1–2. (A lattice of 44 points per side was used throughout.) Fig. 1 shows $\psi_0^2(\vec{r})$, i.e., the square of the ground state eigenfunction, for this “minimally-fused” configuration. Note that $\psi_0^2(\vec{r})$ lies entirely in sphere 1. The first excited state (not shown) is similar in shape, but is entirely confined to sphere 2. In fact, due to the impenetrable walls of the container and the tiny contact region, the eigenstates divide into sets, one set describing a particle in spherical cavity 1 and a second set associated with sphere 2. Because of this character, the monomer densities in spheres 1 and 2 are easily calculated (cf. Eq. (3)), and the partition coefficient is given by:

$$\frac{M_1}{M_2} = \frac{\sum_{j=0}^{\infty} A_j^{(1)2} e^{-ME_j^{(1)}}}{\sum_{j=0}^{\infty} A_j^{(2)2} e^{-ME_j^{(2)}}} \rightarrow \frac{A_0^{(1)2}}{A_0^{(2)2}} e^{-M[E_0^{(1)} - E_0^{(2)}]}, \quad (5)$$

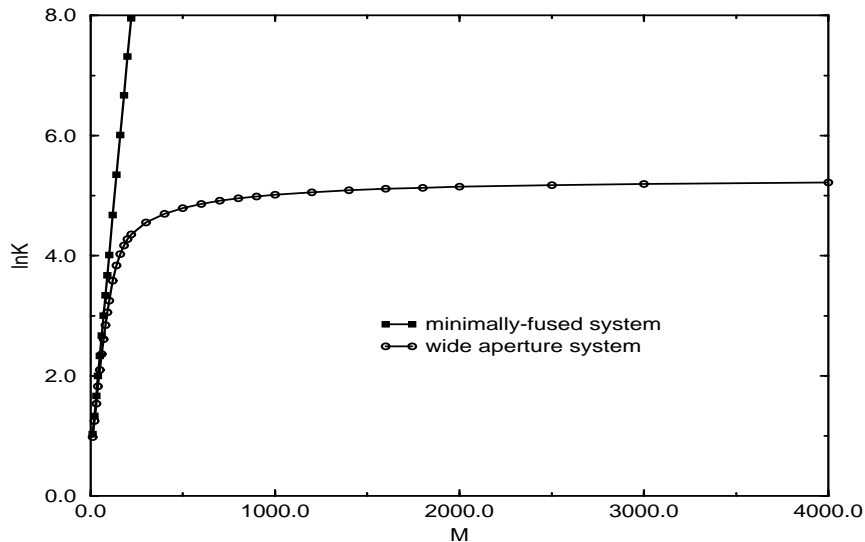


Figure 2: $\ln K$ vs. M for $\lambda = 0.0$. Squares depict result for the minimally-fused aperture system; circles depict the analogous result for the wide aperture system illustrated in Fig. 3.

where the superscript (1) denotes states localized in sphere 1, analogously for (2), and the sums in numerator and denominator are over all states localized in spheres 1 and 2, respectively. The large M limit is indicated by the arrow.

Noting that the ground state energy of a particle in a spherical box of radius R is $E_0 = \pi^2 b^2 / 6R^2$, we see that Eq. (5) is in perfect harmony with the estimation of Muthukumar and Baumgärtner, Eq. (1) (with $\nu = 1/2$). The converged $\ln K$ vs. M curve, shown in Fig. 2, confirms the rapid onset of the limiting behavior prescribed by Eq. (5).

It is interesting to consider the effect of a wider aperture on polymer partitioning between the same two spheres considered above. The specific “wide-aperture” case we will study is shown in Fig. 3 with the two spheres moved inside each other by one more lattice spacing. We expect that the eigenstates of a Hamiltonian with this confining potential will not be completely localized in one sphere or the other. This expectation is born out by explicit numerical calculation. $\psi_0^2(\vec{r})$ is shown in Fig. 3 for the values of R_1 , R_2 and b noted above (which are used in all calculations presented below). Note in particular that the ground state of this fused two-sphere system has some “leakage” into the the smaller

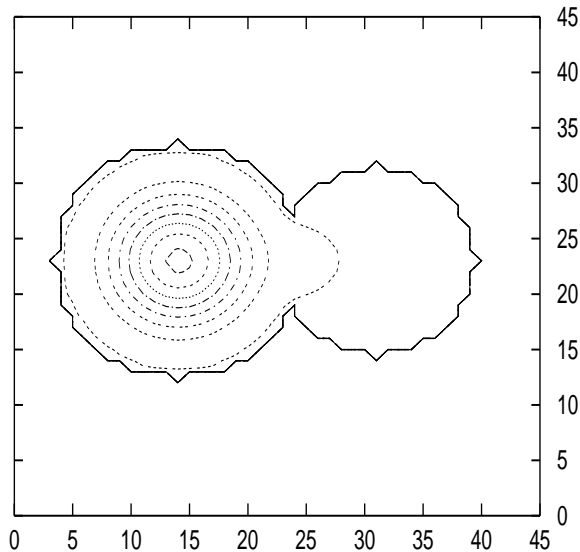


Figure 3: Slice through a plane containing the symmetry axis of two spheres with radii $R_1 = 1.0$ (left) and $R_2 = 0.8$ (right) connected by a wide aperture. Solid line shows outline of the confining system. Also shown, via dashed lines, is a contour plot of $\psi_0^2(\vec{r})$ in this plane for the case of $\lambda = 0.0$ (no excluded volume). Note the leakage of this function into the small sphere.

sphere. This means that in the large polymer chain limit, where the monomer density is determined solely by $\psi_0^2(\vec{r})$, M_1/M_2 saturates at a finite value, as shown in Fig. 2, rather than tending to infinity as it does in the limit of an infinitesimal aperture.

The situation becomes more complicated when excluded volume between monomers is incorporated into the model. Adopting a mean-field description of excluded volume effects leads to the following modification of the quantum-mechanical isomorphism utilized above. Namely, the relevant effective Schrödinger Equation becomes [4],

$$\left[-\frac{b^2}{6} \nabla^2 + \lambda \rho(\vec{r}) \right] \psi(\vec{r}) = E \psi(\vec{r}) . \quad (6)$$

Here $\lambda > 0$ is the excluded volume parameter, which has the dimensions of volume and can be approximately identified with the cube of the monomer radius. Since the effective potential is now a functional of the eigenfunctions of the Hamiltonian operator, a nonlinear Schrödinger Equation must be solved. We do this by an iterative process in which an initial density profile is “guessed” (e.g., the density corresponding to the $\lambda = 0$ limit), the Schrödinger Eq. (6) is solved using the discretized real-space lattice/Lanczos procedure described above, the eigenfunctions and eigenvalues obtained from this calculation are used to compute a new density (via Eq. (3) above), and the cycle is repeated until self-consistency is achieved. In practice, since this Schrödinger Equation is highly nonlinear, care has been taken in order to prevent the onset of numerical instabilities [7].

We considered the same minimally fused system studied above in the $\lambda = 0$ limit for the case $\lambda = 0.001$. The dependence of the natural log of the partition coefficient on polymer length M is shown in Fig. 4. Note that for small M the effects of excluded volume are negligible, i.e., $\ln K$ grows nearly linearly with M , in accord with the $\lambda = 0.0$ case. However, as the polymer length increases, $\ln K$ increases *sublinearly* with M . As M increases further, $\ln K$ reaches a maximum and then begins to *decrease*. At very large M an asymptotic value, bound from below by the natural log of the volume ratio of the two spheres, is obtained. All these features are in agreement with the expectations expressed at the outset, and also consistent with experiments and simulations on a spherical cavity embedded in a gel network, but are not contained in Eq. (1).

An important observation is that for the mean-field excluded volume model considered here, *ground state dominance in the large chain-length limit does not necessarily occur*. In fact, in the present minimally-fused spheres example, the notion of ground state dominance fails manifestly. In the inset to Fig. 4 we plot $\Delta \equiv \exp[-M(E_1 - E_0)]$ vs. M , as an indicator of ground state dominance ($\Delta \rightarrow 0$ as $M \rightarrow \infty$). It can be seen that ground state dominance does not occur in the minimally-fused spheres example. Because the energy levels E_j depend on M in this nonlinear Schrödinger Equation, it is not guaranteed that $M(E_1 - E_0) \gg 1$ as $M \rightarrow \infty$. Explicit calculation shows that the gap between E_0 and E_1 narrows in such a way that this condition never arises. Even in the large M limit the first excited state must be retained in the calculation in order to obtain the correct large M limit of the partition coefficient K .

We have also considered the effect of a wide aperture on the Gaussian polymer with

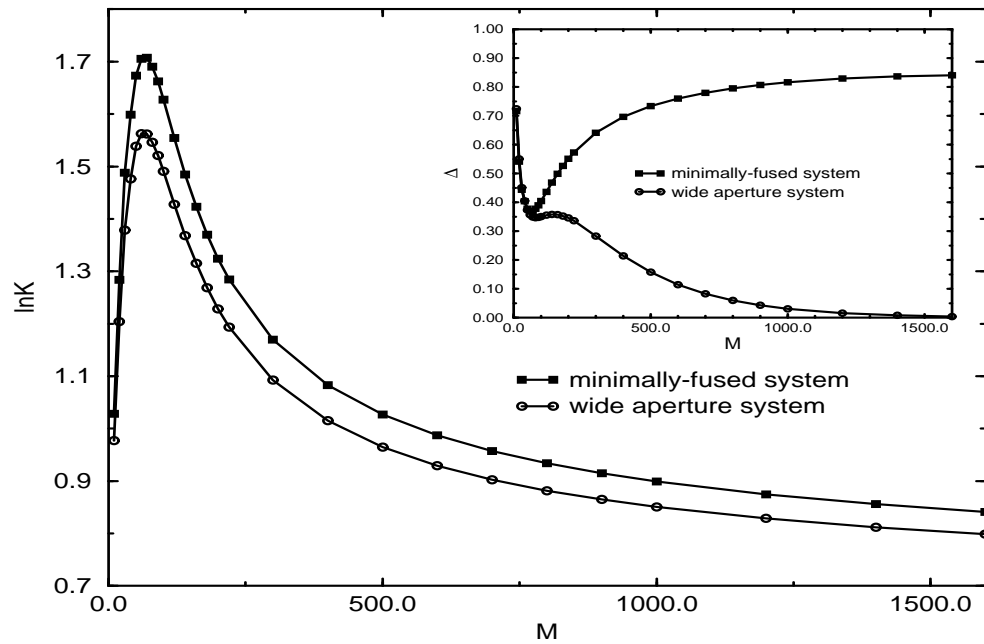


Figure 4: Main panel shows $\ln K$ vs. M for $\lambda = 0.001$. Squares show results for the minimally-fused aperture; circles show analogous results for the wide aperture case. The inset shows the number $\Delta \equiv \exp[-M(E_1 - E_0)]$ as a function of M .

excluded volume. As indicated in the inset to Fig. 4, in this case ground state dominance *does* obtain in the large M limit, consistent with the behavior of a single cavity system (e.g., a single sphere or ellipsoid). The $\ln K$ vs. M curve, shown in the main panel of Fig. 4, has the same generic shape as for the minimally fused case.

In summary, we have used a finite-difference representation of the 3D Schrödinger Equation to compute the equilibrium partition coefficient for a single Gaussian polymer chain in a system consisting of two spheres of unequal sizes connected by a narrow conduit. If excluded volume effects are neglected, this approach provides numerically exact solutions for the Gaussian chain model. Such calculations show that for a very narrow conduit, the estimation previously provided by Muthukumar and Baumgärtner [3] is accurate, while for a wider conduit the partition coefficient saturates at a large but finite value. When excluded volume is included at the mean field level the situation changes considerably. For small M the system shows nearly linear growth of $\ln K$ with M (essentially, excluded volume corrections are unimportant), while for larger M , this curve achieves a maximum and then falls to an asymptote at infinite M which reflects the volume ratio of the two spheres. The possibility of failure of the notion of ground state dominance in this system emphasizes the importance of carefully considering the effects of excited state contributions to the relevant Green's functions, even in the large chain length limit. Extension of this analysis to the case of a charged polymer chain in the presence of electrolyte solution will be considered in subsequent work.

Acknowledgements: We thank Anthony Duncan for many valuable discussions. This work was partially supported by National Science Foundation grant No. CHE-9633561.

References

- [1] D. Rodbard and A. Chrambach, Proc. Nat. Acad. Sci. USA **65**, 970 (1970); G. Guillot, L. Leger and F. Rondelez, Macromolecules **18**, 2531 (1985).
- [2] E. F. Casassa, Polymer Lett. **5**, 773 (1967). E. F. Casassa and Y. Tagami, Macromolecules **2**, 14 (1969).

- [3] A. Baumgärtner and M. Muthukumar, *J. Chem. Phys.* **87**, 3082 (1987); M. Muthukumar and A. Baumgärtner, *Macromolecules* **22**, 1937 (1989).
- [4] P.-G. de Gennes, *Scaling Concepts in Polymer Physics* (Cornell University Press, Ithaca, NY, 1979); M. Doi and S. F. Edwards, *The Theory of Polymer Dynamics* (Clarendon, Oxford, 1986).
- [5] L. Liu, P. Li and S. A. Asher, *Nature* **397**, 141 (1999); L. Liu, P. Li and S. A. Asher, *J. Am. Chem. Soc.*, **121**, 4040 (1999).
- [6] S-S. Chern and R. D. Coalson, *J. Chem. Phys.*, **111**, 1778 (1999).
- [7] S. Tsonchev, R. D. Coalson and A. Duncan, *Phys. Rev. E*, in press.
- [8] G. H. Golub and C. F. Van Loan, *Matrix Computations* (Johns Hopkins University Press, Baltimore, 1996); W. H. Press, B. P. Flannery, S. A. Teukolsky and W. T. Vetterling, *Numerical recipes in C: the art of scientific computing* (Cambridge University Press, 1992).